Monastrol Targeted KIF11 Showed Potential Treatment Effective of Small Cell Lung Cancer

Xinhui Wang (1948706299@qq.com)
Jilin University First Hospital https://orcid.org/0000-0001-7397-3469
Shanshan Jiang
China Academy of Information and Communications Technology
Baolin Zhou
Xinxiang Medical University First Affiliated Hospital
Zhantao Liu
Jilin University First Hospital
Ziling Liu
Jilin University First Hospital

Research article

Keywords: bioinformatics; lung science; SCLC; Monastrol

Posted Date: November 19th, 2019

DOI: https://doi.org/10.21203/rs.2.17513/v1

Abstract

Objective: This study is to identify Small Cell Lung Cancer (SCLC) driver genes, annotate enrichment functions and key pathways, and also verify Monastrol therapeutic effect. Methods: The gene expression profiles of GSE40275 and GSE43346 was analyzed to identify the DEGs (Differentially Expressed Genes) between SCLC and the normal tissue. GO (Gene Ontology), KEGG (Kyoto Encyclopedia of Genes and Genomes) analysis and PPI (Protein-protein interaction) network analysis were conducted to find out the enrichment functions, pathways and hub genes. Moreover, in vitro, MTT assay, colony-forming assay, and the scratch assay were performed to verify the effect of Monastrol. Results: There were common 129 up-regulated and 176 down-regulated DEGs between SCLC samples and normal lung samples. KIF11, NDC80 and PBK were identified as hub genes after PPI network analysis. The q-PCR results showed that genes KIF11, NDC80 and PBK consistently expressed higher in cancer cells than normal cell lines. And in vitro assay showed that Monastrol inhibited SCLC cellular viability, proliferation and migration ($P < 0.01$). Conclusion: KIF11, NDC80 and PBK were aberrantly expressed and could be potentially applied as diagnostic biomarkers, therapeutic targets and prognostic biomarkers. Monastrol was a promising drug in treatment of SCLC patients. Key words: bioinformatics; lung science; SCLC; Monastrol.

Background

Lung cancer, one of the leading causes of cancer-related deaths worldwide, is the most common type of cancer in men and the fourth most common in women[1]. Small cell lung cancer (SCLC) with high degree of malignancy and high mortality is account for about 13-20% of all lung cancer cases. In the developed countries such as the United States, SCLC is estimated to represent about 16% of new lung cancer diagnoses, which means that about 35,000 new cases occur annually[2]. In underdeveloped countries, the percentage of SCLC cases is higher. More than 130,000 new diagnoses of SCLC and 100,000 deaths from this disease were estimated to have occurred in China in 2013[3].

Small cell cancer is highly aggressive. This kind of tumor cells is characterized by rapid doubling time and not suitable for traditional surgical therapy but sensitive to both chemotherapy and radiation. Unfortunately, these conventional treatment methods are both short in duration and not curative in most cases with an average 5-year survival rate below 7%. No major treatment advances have occurred over the past 30 years[4]. In patients with extensive-stage disease, chemotherapy alone can palliate symptoms and prolong survival in most patients; however, long-term survival is rare[5]. The management of SCLC is still very challenging cause of disease outcome has remains stubbornly poor due mainly to limited options for effective treatment. Although according to some preclinical studies about the understanding of SCLC, the c-kit inhibitor and other agents targeting angiogenesis could show an inhibition on it, the results of the actual use were somewhat disappointing and unexpected. Meanwhile, there is no clear expatiation about the neoplastic processes of SCLC[6]. In this way, conducting such a study which comprehensively depicts molecular pathogenesis of SCLC development as well as identifies novel therapeutic agents is necessary and crucial.

The hallmarks of cancer are the most crucial to the development of SCLC, including genomic instability and mutations, evading growth suppressors, resisting cell deaths, sustaining proliferative signaling and enabling replicative immorality. The genomic instability of SCLC is higher than most cancers. SCLC has a mutation rate with 5.6 to 7.4 mutations per Mb, and about 175 mutations per tumor[7]. However, few specific driver genes have been proved related to SCLC pathogenesis. To further clarify the molecular pathogenesis of this tumor, our study also used bioinformatics methods combining with GO, KEGG analysis and PPI network analysis, employing mRNA microarray datasets to screen out the hub genes and key pathways associated with SCLC.

Methods

Microarray data

The gene expression profiles of GSE40275 and GSE43346 were collected from GEO database (The Gene Expression Omibus, http://www.ncbi.nlm.nih.gov/geo). These profiles contained 40 SCLC samples and 44 normal samples totally.

Identification of DEGs

The analysis was conducted based on raw data using software GeneSpring (version 11.5, Aglient, USA). The category of the mRNA expression data was realized with hierarchical clustering analysis. The probe quality control in GeneSpring was limited by virtue of principal component analysis (PCA), and probes with intensity values below 20th percentile were filtered out using the “filter probesets by expression” option. Then, the DEGs were identified using classical t test with P value cutoff of <0.05 and a change >2 fold, which were applied for statistically significant definition. At last, the Venn plot analysis regarding DEGs was conducted (http://bioinformatics.psb.ugent.be/webtools/Venn/).

Gene ontology and pathway enrichment analysis of DEGs

The DAVID database (Database for Annotation, Visualization and Intergrated Discovery, http://david.abcc.ncifcrf.gov/), provided a comprehensive set of functional annotation tools to understand biological meaning underlying plenty of genes. GO (Gene Ontology) was a useful method for analyzing biological process, molecular function and cell component of genes. And KEGG (Kyoto encyclopedia of Genes and Genomes) was a base for gene function analysis and genomic information link. In this study, GO and KEGG pathway enrichment analysis were performed using DAVID for DEGs functions analysis.

PPI network construction and modules selection

STRING (Search Tool for Retrieval of Interacting Genes, http://string.embl.de/) can provide PPI (Protein-Protein Interaction) analysis for bioinformatic studies. Then, the software Cytoscape was applied to screen hub genes and modules with MCODE (Molecular Complex Detection). Moreover, the function and pathway enrichment analysis of DEGs in modules were performed.

Cell lines and reagents

Human normal pulmonary epithelial cells (BEAS-2B), human normal embryonic lung fibroblast cells (MRC5), human small cell lung cancer cells (H446) and human lung adenocarcinoma cells (A549) were purchased from the ATCC (American Type Culture Collection). Those cell lines were cultured in Dulbecco's modified Eagle's medium (DMEM, Hyclone, USA) supplemented with 10% fetal bovine serum (FBS, Gibco, USA). These cells were cultivated in 5% CO_2 and 95% air at 37°C. And Monastrol, the small molecule inhibitor, was purchased from Apexbio Inc. (Apexbio, Houston, USA).

Real-time quantitative reverse transcription PCR

Aim to confirm the expression of hub genes in SCLC cell lines and normal human pneumonocytes, we performed qRT-PCR using FastStart Universal SYBR Green Master (ROX) (Roche Diagnostics) in a CFX96 Real-Time System (Bio-Red) according to the manufacturer's instructions and expression levels were normalized to glyceraldehyde-3-phosphate dehydrogenase (GAPDH). The $2^{-\triangle\triangle Ct}$ method was used for qRT-PCR data analysis.

MTT assay

The cancer cells (H446, A549) and normal cells (BEAS-2B, MRC5) were plated into 96-well culture plate with a density of 500 cells/well, and were treated with different doses of Monastrol respectively. The MTT reagent (Sigma) was dissolved in PBS (5mg/ml) to measure the viability of cells. On the day of measurement, medium was replaced on fresh DMEM supplemented with 10% FBS and diluted MTT (1:10, 10% MTT), and incubated for 3, 5 hours at 37°C. Then, the incubation medium was removed and formazan crystals were dissolved in 200μl solution of DMSO. The ELx800 absorbance microplate reader (BioTek Instruments, VT, USA) was applied to quantify the MTT reduction by measuring the light absorbance at 570nm. Each test was repeated 3 times.

Colony-forming assay

The cancer cells (H446, A549) were cultured in Petri dishes with 50 cells/cm^2. After 24 hours, those cells were treated with different doses of Monastrol respectively. After ten days in vitro growth, colonies were counted. Then, colonies were rinsed with PBS, fixed in 4% paraformaldehyde, stained with 5% crystal violet for half hours, and rinsed twice with water.

In vitro scratch assay

The H446 and A549 cells were cultured on 24-well Permanox^{TM} plates. A 1ml pipette tip across each well was used to creat a consistent cell-free area. The loose cells were washed out gently using DMEM. Then, the cells were exposed to different doses of Monastrol. After the scratch and at 0, 12, 24 hours, the images of the scraped area were captured with phase contrast microscopy. The remaining wounded area and the scratch width at six different points per image were measured.

Statistical analysis

All statistic data were entered into SPSS 20.0 (SPSS Inc., Chicago, Illinois, USA) for analysis. Independent-samples t test was conducted to analyze quantitive data. P values < 0.05 were set as significance level.

Results

Indentification of DEGs and gene function analysis

The gene expression level of GSE40275 and GSE43346 were showen in the volcano plots (**Figure 1A**). Altogether 305 DEGs were picked up between normal and SCLC mRNA expression samples shown in the VENN plots (**Figure 1B**). The mutual DEGs were uploaded to DAVID respectively, to identify the further insight of those genes. The detailed results of GO and KEGG pathway analysis were showed in **Table 1** and **Figure 1C**. The GO and KEGG analysis results revealed that the mutual up-regulated DEGs were mainly associated with cell division, nucleoplasm, protein binding and Cell cycle. Meanwhile, for the mutual down-regulated DEGs, the GO and KEGG analysis results primarily enriched in immune response, plasma membrane, scavenger receptor activity and Complement and coagulation cascades.

Module screening from the PPI network

All DEGs among these samples were analyzed with PPI network, and the hub genes were screened with degrees > 90 based on the STRING database. Top 20 genes were identified as hub genes listed in **Table 2**. And heat maps of these hub genes expressions were showed in **Figure 3A**. Among those genes, the node

degree of TOP2A was the highest one, which degree was 112. Moreover, after MCODE analysis, the top 3 significant modules were obtained, showed in **Figure 2**. The functional annotation and enrichment of these modules were also performed, showed in **Table 3**. Enriched function analysis revealed that genes in module 1 were primarily related to protein binding, cell division and Cell cycle. In module 2-3, genes were mainly enriched in inflammatory response, Chemokine signaling pathway and cellular defense response.

Validation of common hub genes by qRT-PCR

To validate the expression of KIF11, NDC80, PBK and TOP2A in human normal lung cells (BEAS-2B, MRC5), human small cell lung cancer cells (H446) and human lung adenocarcinoma cells (A549), qRT-PCR was performed. The results, showed in **Figure 4A**, revealed among those cell lines that genes KIF11, NDC80, PBK and TOP2A consistently expressed higher in cancer cells than normal cell lines ($P < 0.05$).

Monastrol reduces proliferation of SCLC cells

To evaluate the sensitivity of lung cancer cells to Monastrol, the survival cells after treatment were calculated by MTT assay. As showed in **Figure 4B**, following the augment of drug concentrations, the cellular viabilty (ratio to control) in cell lines H446 and A549 decreased significantly. However, BEAS-2B and MRC5 still had a high cellular viability even subjected to the highest doze. Monastrol was relatively tolerated for normal lung cells lines. To determine the anti-cancer effects of Monastrol in SCLC cells, we performed colony-forming assay. The results showed us that less and smaller clonogenicities in Petri dishes with Monastrol than that in control group (**Figure 4C**). The percentage of clone formation in control was significantly higher than in drug groups (0.25μmol/L, 1μmol/L).

Monastrol inhibits migration of SCLC cells

The widths of scratched areas were measured after the scratch, after 12h, and after 24h, to research the migration of SCLC cells. In **Figure 4D**, the width of scratched was significantly smaller after 24h in control group. However, there was only a slight decrease in Monastrol group. In addition, after 24h, the wounds in control group were also smaller than in drug group significantly.

Discussion

SCLC often diagnosed in an advanced stage, which is a highly aggressive malignancy associated with early metastasis, rapid progression, and poor survival. First line chemotherapy provides good response rates in advanced disease, but SCLC often relapses, progression free and overall survival are limited. Few

related genes and molecular pathways have been studied by previous researchers, there is an urgent need for comprehensive analysis regarding to SCLC[8, 9]. And clinical diagnosis, treatment and prognosis would be significantly improved if the appropriate targets are identified. Our study used bioinformatics analysis techniques combined with complicated and refined algorithm to identify key genes and pathways, which could provide potential targets for SCLC diagnosis and treatment. And screening anti-SCLC drugs based on targets to improve clinical treatment.

GSE40275 and GSE43346 datasets were downloaded, and then we screened normal tissues and SCLC tissues samples from them, also identified the DEGs between normal tissues and SCLC tissues. Result showed that there were 305 DEGs, 129 up-regulated and 176 down-regulated. The functions and corresponding signaling pathways of DEGs were investigated by GO and KEGG analysis. The cell division and sister chromatid cohesion biological process are up-regulated observably, at the same time, the ratios of nucleus related components up-regulated obviously. These changes may favor the preparation for DNA replication and promote the self-duplication of SCLC cells. The infinite proliferation of tumor cells is actually the abnormality of cell division and might be the result of Insensitivity to Antigrowth Signals. The signal pathway of Oocyte meiosis abnormal activation suggests that there is a difference in the incidence of SCLC between men and women. Meanwhile, the formation of neovascularization is closely related to the development of tumor, Fanconi anemia pathway exceeding activation plays an important role in the occurrence and development of SCLC. The positive regulation of vasoconstriction is down-regulated, and the continuous supply of blood flow is related to the need for adequate blood supply for the growth of tumor tissue. The changes of extracellular membrane components regulate the recognition and signal transmission between tumor cells, and promote the migration of tumor cells at the same time. At the same time, the scavenger receptor activity is suppressed that may cause body unable to recognize and remove abnormal cells, leading to carcinogenesis, and then SCLC occurs. These results further explain the tumor formation mechanism of SCLC, and also provide novel ideas for further study of SCLC in the future.

PPI network of DEGs was constructed using STRING database and Cytocape. Three hub genes (KIF11, NDC80 and PBK) were identified as driver genes closely related to SCLC development and they had never been reported related to SCLC in previous studies. KIF11, kinesin family member 11, located in Chr10q23.33, encodes a motor protein which is known to be involved in spindle assembly, control mitotic spindle structure and chromosome behaviour during mitosis[10, 11]. The function of this protein includes chromosome positioning, centrosome separation and establishing a bipolar spindle during cell mitosis. Kinesin motor domains couple cycles of ATP hydrolysis to cycles of microtubule binding and conformational changes that result in directional force and movement on microtubules[12]. Meanwhile, KIF11 dephosphorylation can led to mitotic exit, and the expression level of this gene is low in normal lung tissue[13, 14]. In SCLC cells, overexpression of this gene may lead to a rise in phosphorylated Erk1/2 levels, promote bipolar spindle assembly and chromosome segregation[15-17]. And this gene also plays a

role in DNA repair, gives assistance for some protein's transport from the trans-Golgi network to the cell surface and contributes to mitotic spindle checkpoint activation and Tat-mediated apoptosis in CD4-positive T-lymphocytes, which may boosts the progress of small cell lung cancer development. Given these circumstances, KIF11 might be a potential microtubule-related target for proliferating SCLC cells[18-21]. It prompted us to hypothesize that Monastrol, a potent and cell-permeable inhibitor targeted KIF11 with an IC_{50} value of 14 μM, which causes aberrant interactions with the microtubule, and reversals at the ATP hydrolysis step, might have anti-SCLC therapeutic effects[22-24]. And it had also been verified by the following assays in this studies. The drug in protein binding structure 1X88 was downloaded in PDB dataset (Protein data bank, http://www.rcsb.org/), and shown in **Figure3B**.

NDC80, kinetochore complex component, located in Chr18p11.32, encoded protein consists of an N-terminal microtubule binding domain and a C-terminal coiled-coiled domain that interacts with other components of NDC80 kinetochore complex, which directly modulates microtubule dynamics[25]. This protein functions to organize and stabilize microtubule-kinetochore interactions and is required for proper chromosome segregation. Aurora A kinase phosphorylates NDC80 to regulate metaphase kinetochore-microtubule dynamics[26]. And Aurora B-NDC80-Mps1 signaling axis is governing accurate chromosome segregation in mitosis[27]. Overproduction of Ndc80 in cancer cells unfavourably absorb protein interactors through the internal loop domain and lead to a change in the equilibrium of microtubule-associated proteins[28]. NDC80's interaction with either growing or shrinking microtubule ends such as differentially regulates mammalian kinetochore coupling to polymerizing and depolymerizing microtubules can be tuned by the phosphorylation state of its tail[29, 30]. N-terminus-modified NDC80 can suppress tumour growth by interfering with kinetochore-microtubule dynamics[31]. In our study, it showed that this gene, which was the core of the interaction with multiple genes, had a pivotal position in SCLC tissues. The expression of this gene was abnormal regulated, in view of NDC80 was a driver gene of SCLC, we hypothesized its abnormal activation would promote the initiation of SCLC, it might play an important role during the course of SCLC development and it might be a biomarker in the early diagnosis of SCLC. Accordingly, NDC80 could be considered as an important therapeutic target for SCLC.

PBK, PDZ binding kinase, this gene locates at Chr8p21.1 and encodes a serine/threonine protein kinase related to the dual specific mitogen-activated protein kinase kinase (MAPKK) family. This kinase can increase the rate of mitosis and expands malignant T cells[32]. FoxM1-regulated PBK exerts oncogenic activities via the activation of beta-Catenin pathway[33]. CDK1-mediated mitotic phosphorylation of PBK is involved in cytokinesis and inhibits its oncogenic activity[34]. PBK promotes lung cancer resistance to EGFR tyrosine kinase inhibitors by phosphorylating and activating c-Jun[35]. PBK mediates promyelocyte proliferation via Nrf2-regulated cell cycle progression and apoptosis[36].
TOPK/PBK promotes cell migration via modulation of the PI3K/PTEN/AKT pathway and is associated with poor prognosis in lung cancer[37]. Increased levels of PBK may contribute to tumor cell development and progression through suppression of p53 function and consequent reductions in the cell-cycle regulatory proteins such as p21[38]. PBK augments tumor cell growth following transient appearance in

different types of progenitor cells in vivo as reported[39]. Overexpression of this gene has been implicated in tumorigenesis. Overexpression of PBK contributes to tumor development and poor outcome of SCLC[40]. PBK might play a pivotal role in SCLC invasion and metastasis[41]. Our research confirms that the expression of this gene was abnormal regulated and it is a core driver gene of SCLC.

The effects of Monastrol were evaluated in present study with MTT assay, colony-forming assay, and scratch assay in vitro. In MTT assay, the cellular viability (ratio to control) in H446 and A549 cell lines were revealed dose-depended decreased when treated with Monastrol. In colony-forming assay, the numbers and size of clonogenicities in Monastrol group were significantly less than control group, which was consistent with the results that Monastrol can reduce the proliferation of SCLC cells. In scratch assay, the wound widths in control group decreased sharply along with time, and were smaller than that in Monastrol group after 48h significantly. That implied that Monastrol strongly inhibited migration of SCLC cells. All these results suggest that Monastrol have the potential effect for treating SCLC, which is worthy of further study.

Conclusions

Our study selected out the DEGs and key pathways in the NFPA tissue. The DEGs identified in this study provided comprehensive insight into the molecular mechanism of the SCLC pathogenesis. Three hub genes: KIF11, NDC80 and PBK were aberrantly expressed and could be potentially applied as diagnostic biomarkers, therapeutic targets and prognostic biomarkers. Meanwhile, Monastrol, a potent inhibitor regarding to KIF11, suppressed proliferation and migration of SCLC cells, was a promising drug in treatment of SCLC patients.

Declarations

Compliance with ethical standards

Conflict of interest The authors declare that they have no conficts of interest (including fnancial and non-fnancial interests).

Ethical approval All procedures performed in studies involving human participants were in accordance with the ethical standards of the institutional and/or national research committee and its later amendments or comparable ethical standards.

References

[1] Stumpf C, Kaemmerer D, Neubauer E, Sanger J, Schulz S, Lupp A. Somatostatin and CXCR4 expression patterns in adenocarcinoma and squamous cell carcinoma of the lung relative to small cell lung cancer. 2018;144(10):1921-1932.

[2] Zhao H, Ren D, Liu H, Chen J. Comparison and discussion of the treatment guidelines for small cell lung cancer. 2018;9(7):769-774.

[3] Bunn PA, Jr., Minna JD, Augustyn A, Gazdar AF, Ouadah Y, Krasnow MA, Berns A, Brambilla E, Rekhtman N, Massion PP, Niederst M, Peifer M, Yokota J, Govindan R, Poirier JT, Byers LA, Wynes MW, McFadden DG, MacPherson D, Hann CL, Farago AF, Dive C, Teicher BA, Peacock CD, Johnson JE, Cobb MH, Wendel HG, Spigel D, Sage J, Yang P, Pietanza MC, Krug LM, Heymach J, Ujhazy P, Zhou C, Goto K, Dowlati A, Christensen CL, Park K, Einhorn LH, Edelman MJ, Giaccone G, Gerber DE, Salgia R, Owonikoko T, Malik S, Karachaliou N, Gandara DR, Slotman BJ, Blackhall F, Goss G, Thomas R, Rudin CM, Hirsch FR. Small Cell Lung Cancer: Can Recent Advances in Biology and Molecular Biology Be Translated into Improved Outcomes? Journal of thoracic oncology : official publication of the International Association for the Study of Lung Cancer. 2016;11(4):453-474.

[4] Byers LA, Rudin CM. Small cell lung cancer: where do we go from here? Cancer. 2015;121(5):664-672.

[5] Kalemkerian GP, Akerley W, Bogner P, Borghaei H, Chow LQ, Downey RJ, Gandhi L, Ganti AK, Govindan R, Grecula JC, Hayman J, Heist RS, Horn L, Jahan T, Koczywas M, Loo BW, Jr., Merritt RE, Moran CA, Niell HB, O'Malley J, Patel JD, Ready N, Rudin CM, Williams CC, Jr., Gregory K, Hughes M. Small cell lung cancer. Journal of the National Comprehensive Cancer Network : JNCCN. 2013;11(1):78-98.

[6] Pillai RN, Owonikoko TK. Small cell lung cancer: therapies and targets. Seminars in oncology. 2014;41(1):133-142.

[7] Waqar SN, Morgensztern D. Treatment advances in small cell lung cancer (SCLC). Pharmacology & therapeutics. 2017;180:16-23.

[8] Hendriks LEL, Menis J, Reck M. Prospects of targeted and immune therapies in SCLC. Expert review of anticancer therapy. 2018:1-17.

[9] Wang Z, Fu S, Zhao J, Zhao W, Shen Z, Wang D, Duan J, Bai H, Wan R, Yu J, Wang S, Chen H, Chen B, Wang L, Wang J. Transbronchoscopic patient biopsy-derived xenografts as a preclinical model to explore chemorefractory-associated pathways and biomarkers for small-cell lung cancer. Cancer letters. 2019;440-441:180-188.

[10] Duan Y, Huo D, Gao J, Wu H, Ye Z, Liu Z, Zhang K, Shan L, Zhou X, Wang Y, Su D, Ding X, Shi L, Wang Y, Shang Y, Xuan C. Ubiquitin ligase RNF20/40 facilitates spindle assembly and promotes breast carcinogenesis through stabilizing motor protein Eg5. Nature communications. 2016;7:12648.

[11] He J, Zhang Z, Ouyang M, Yang F, Hao H, Lamb KL, Yang J, Yin Y, Shen WH. PTEN regulates EG5 to control spindle architecture and chromosome congression during mitosis. Nature communications. 2016;7:12355.

[12] Scarabelli G, Grant BJ. Kinesin-5 allosteric inhibitors uncouple the dynamics of nucleotide, microtubule, and neck-linker binding sites. Biophysical journal. 2014;107(9):2204-2213.

[13] Liu Y, Zhang Z, Liang H, Zhao X, Liang L, Wang G, Yang J, Jin Y, McNutt MA, Yin Y. Protein Phosphatase 2A (PP2A) Regulates EG5 to Control Mitotic Progression. Scientific reports. 2017;7(1):1630.

[14] Fagerberg L, Hallstrom BM, Oksvold P, Kampf C, Djureinovic D, Odeberg J, Habuka M, Tahmasebpoor S, Danielsson A, Edlund K, Asplund A, Sjostedt E, Lundberg E, Szigyarto CA, Skogs M, Takanen JO, Berling H, Tegel H, Mulder J, Nilsson P, Schwenk JM, Lindskog C, Danielsson F, Mardinoglu A, Sivertsson A, von Feilitzen K, Forsberg M, Zwahlen M, Olsson I, Navani S, Huss M, Nielsen J, Ponten F, Uhlen M. Analysis of the human tissue-specific expression by genome-wide integration of transcriptomics and antibody-based proteomics. Molecular & cellular proteomics : MCP. 2014;13(2):397-406.

[15] Imai T, Oue N, Nishioka M, Mukai S, Oshima T, Sakamoto N, Sentani K, Matsusaki K, Yoshida K, Yasui W. Overexpression of KIF11 in Gastric Cancer with Intestinal Mucin Phenotype. Pathobiology : journal of immunopathology, molecular and cellular biology. 2017;84(1):16-24.

[16] van Heesbeen RG, Tanenbaum ME, Medema RH. Balanced activity of three mitotic motors is required for bipolar spindle assembly and chromosome segregation. Cell reports. 2014;8(4):948-956.

[17] Gayek AS, Ohi R. Kinetochore-microtubule stability governs the metaphase requirement for Eg5. Molecular biology of the cell. 2014;25(13):2051-2060.

[18] Tan LJ, Saijo M, Kuraoka I, Narita T, Takahata C, Iwai S, Tanaka K. Xeroderma pigmentosum group F protein binds to Eg5 and is required for proper mitosis: implications for XP-F and XFE. Genes to cells : devoted to molecular & cellular mechanisms. 2012;17(3):173-185.

[19] Wakana Y, Villeneuve J, van Galen J, Cruz-Garcia D, Tagaya M, Malhotra V. Kinesin-5/Eg5 is important for transport of CARTS from the trans-Golgi network to the cell surface. The Journal of cell biology. 2013;202(2):241-250.

[20] Liu M, Li D, Sun L, Chen J, Sun X, Zhang L, Huo L, Zhou J. Modulation of Eg5 activity contributes to mitotic spindle checkpoint activation and Tat-mediated apoptosis in CD4-positive T-lymphocytes. The Journal of pathology. 2014;233(2):138-147.

[21] Hayashi N, Koller E, Fazli L, Gleave ME. Effects of Eg5 knockdown on human prostate cancer xenograft growth and chemosensitivity. The Prostate. 2008;68(12):1283-1295.

[22] Rose AS, Bradley AR, Valasatava Y, Duarte JM, Prlic A, Rose PW. NGL viewer: web-based molecular graphics for large complexes. Bioinformatics (Oxford, England). 2018;34(21):3755-3758.

[23] Cochran JC, Gatial JE, 3rd, Kapoor TM, Gilbert SP. Monastrol inhibition of the mitotic kinesin Eg5. The Journal of biological chemistry. 2005;280(13):12658-12667.

[24] Garcia-Saez I, DeBonis S, Lopez R, Trucco F, Rousseau B, Thuery P, Kozielski F. Structure of human Eg5 in complex with a new monastrol-based inhibitor bound in the R configuration. The Journal of biological chemistry. 2007;282(13):9740-9747.

[25] Umbreit NT, Gestaut DR, Tien JF, Vollmar BS, Gonen T, Asbury CL, Davis TN. The Ndc80 kinetochore complex directly modulates microtubule dynamics. Proceedings of the National Academy of Sciences of the United States of America. 2012;109(40):16113-16118.

[26] DeLuca KF, Meppelink A. Aurora A kinase phosphorylates Hec1 to regulate metaphase kinetochore-microtubule dynamics. 2018;217(1):163-177.

[27] Zhu T, Dou Z, Qin B, Jin C, Wang X, Xu L, Wang Z, Zhu L, Liu F, Gao X, Ke Y, Wang Z, Aikhionbare F, Fu C, Ding X, Yao X. Phosphorylation of microtubule-binding protein Hec1 by mitotic kinase Aurora B specifies spindle checkpoint kinase Mps1 signaling at the kinetochore. The Journal of biological chemistry. 2013;288(50):36149-36159.

[28] Tang NH, Toda T. MAPping the Ndc80 loop in cancer: A possible link between Ndc80/Hec1 overproduction and cancer formation. BioEssays : news and reviews in molecular, cellular and developmental biology. 2015;37(3):248-256.

[29] Alushin GM, Musinipally V, Matson D, Tooley J, Stukenberg PT, Nogales E. Multimodal microtubule binding by the Ndc80 kinetochore complex. Nature structural & molecular biology. 2012;19(11):1161-1167.

[30] Long AF, Udy DB, Dumont S. Hec1 Tail Phosphorylation Differentially Regulates Mammalian Kinetochore Coupling to Polymerizing and Depolymerizing Microtubules. Current biology : CB. 2017;27(11):1692-1699.e1693.

[31] Orticello M, Fiore M, Totta P, Desideri M, Barisic M, Passeri D, Lenzi J, Rosa A, Orlandi A, Maiato H, Del Bufalo D, Degrassi F. N-terminus-modified Hec1 suppresses tumour growth by interfering with kinetochore-microtubule dynamics. Oncogene. 2015;34(25):3325-3335.

[32] Ishikawa C, Senba M, Mori N. Mitotic kinase PBK/TOPK as a therapeutic target for adult Tcell leukemia/lymphoma. International journal of oncology. 2018;53(2):801-814.

[33] Yang YF, Pan YH, Cao Y, Fu J, Yang X, Zhang MF, Tian QH. PDZ binding kinase, regulated by FoxM1, enhances malignant phenotype via activation of beta-Catenin signaling in hepatocellular carcinoma. Oncotarget. 2017;8(29):47195-47205.

[34] Stauffer S, Zeng Y, Zhou J, Chen X, Chen Y, Dong J. CDK1-mediated mitotic phosphorylation of PBK is involved in cytokinesis and inhibits its oncogenic activity. Cellular signalling. 2017;39:74-83.

[35] Li Y, Yang Z, Li W, Xu S, Wang T, Wang T, Niu M, Zhang S, Jia L, Li S. TOPK promotes lung cancer resistance to EGFR tyrosine kinase inhibitors by phosphorylating and activating c-Jun. Oncotarget.

2016;7(6):6748-6764.

[36] Liu Y, Liu H, Cao H, Song B, Zhang W, Zhang W. PBK/TOPK mediates promyelocyte proliferation via Nrf2-regulated cell cycle progression and apoptosis. Oncology reports. 2015;34(6):3288-3296.

[37] Shih MC, Chen JY, Wu YC, Jan YH, Yang BM, Lu PJ, Cheng HC, Huang MS, Yang CJ, Hsiao M, Lai JM. TOPK/PBK promotes cell migration via modulation of the PI3K/PTEN/AKT pathway and is associated with poor prognosis in lung cancer. Oncogene. 2012;31(19):2389-2400.

[38] Hu F, Gartenhaus RB, Eichberg D, Liu Z, Fang HB, Rapoport AP. PBK/TOPK interacts with the DBD domain of tumor suppressor p53 and modulates expression of transcriptional targets including p21. Oncogene. 2010;29(40):5464-5474.

[39] Nandi AK, Ford T, Fleksher D, Neuman B, Rapoport AP. Attenuation of DNA damage checkpoint by PBK, a novel mitotic kinase, involves protein-protein interaction with tumor suppressor p53. Biochemical and biophysical research communications. 2007;358(1):181-188.

[40] Ohashi T, Komatsu S, Ichikawa D, Miyamae M, Okajima W, Imamura T, Kiuchi J, Nishibeppu K, Kosuga T, Konishi H, Shiozaki A, Fujiwara H, Okamoto K, Tsuda H, Otsuji E. Overexpression of PBK/TOPK Contributes to Tumor Development and Poor Outcome of Esophageal Squamous Cell Carcinoma. Anticancer research. 2016;36(12):6457-6466.

[41] Seol MA, Park JH, Jeong JH, Lyu J, Han SY, Oh SM. Role of TOPK in lipopolysaccharide-induced breast cancer cell migration and invasion. Oncotarget. 2017;8(25):40190-40203.

Abbreviations

Biological processes, BP;

Cell component, CC;

Control, CON;

Database for Annotation, Visualization and Intergrated Discovery, DAVID;

Differential expressed genes, DEG;

Dulbecco’s modified Eagle’s medium, DMEM;

Fetal bovine serum, FBS;

Gene Expression Omnibus, GEO;

Gene ontology, GO;

Glyceraldehyde-3-phosphate dehydrogenase, GAPDH;

Human lung adenocarcinoma cells, A549;

Human normal embryonic lung fibroblast cells, MRC5;

Human normal pulmonary epithelial cells, BEAS-2B;

Human small cell lung cancer cells, H446;

Kinesin family member 11, KIF11;

Kinetochore complex component, NDC80;

Kyoto encyclopedia of Genes and Genomes, KEGG;

Molecular Complex Detection, MCODE;

Molecular function, MF;

PDZ binding kinase, PBK;

Principal component analysis, PCA;

Progress free survival, PFS;

Protein-protein interation, PPI;

Search Tool for Retrieval of Interacting Genes, STRING;

Small Cell Lung Cancer, SCLC;

Tables

Table 1 Functional and pathway enrichment analysis of DEGs in SCLC

Functional and pathway enrichment analysis of DEGs in SCLC

Expression	Category	Term	Count	%	PValue
up-regulated	GOTERM_BP_DIRECT	GO:0051301~cell division	37	28.91	7.54E-32
	GOTERM_BP_DIRECT	GO:0007067~mitotic nuclear division	28	21.88	1.72E-24
	GOTERM_BP_DIRECT	GO:0006260~DNA replication	22	17.19	3.46E-21
	GOTERM_BP_DIRECT	GO:0007062~sister chromatid cohesion	17	13.28	2.45E-17
	GOTERM_BP_DIRECT	GO:0000082~G1/S transition of mitotic cell cycle	14	10.94	3.99E-13
	GOTERM_CC_DIRECT	GO:0005654~nucleoplasm	71	55.47	1.59E-26
	GOTERM_CC_DIRECT	GO:0005634~nucleus	87	67.97	2.70E-20
	GOTERM_CC_DIRECT	GO:0030496~midbody	16	12.50	8.93E-15
	GOTERM_CC_DIRECT	GO:0005819~spindle	15	11.72	7.88E-14
	GOTERM_CC_DIRECT	GO:0000777~condensed chromosome kinetochore	13	10.16	5.98E-13
	GOTERM_MF_DIRECT	GO:0005515~protein binding	101	78.91	1.97E-14
	GOTERM_MF_DIRECT	GO:0005524~ATP binding	40	31.25	9.95E-14
	GOTERM_MF_DIRECT	GO:0019901~protein kinase binding	18	14.06	8.97E-10
	GOTERM_MF_DIRECT	GO:0003777~microtubule motor activity	10	7.81	4.15E-09
	GOTERM_MF_DIRECT	GO:0008017~microtubule binding	13	10.16	2.20E-08
	KEGG_PATHWAY	hsa04110:Cell cycle	16	12.50	9.02E-16
	KEGG_PATHWAY	hsa03030:DNA replication	8	6.25	2.68E-09
	KEGG_PATHWAY	hsa03430:Mismatch repair	7	5.47	5.91E-09
	KEGG_PATHWAY	hsa04114:Oocyte meiosis	9	7.03	5.59E-07
	KEGG_PATHWAY	hsa03460:Fanconi anemia pathway	6	4.69	2.42E-05
down-regulated	GOTERM_BP_DIRECT	GO:0050900~leukocyte migration	10	5.85	2.52E-06
	GOTERM_BP_DIRECT	GO:0045907~positive regulation of vasoconstriction	6	3.51	1.21E-05
	GOTERM_BP_DIRECT	GO:0006955~immune response	15	8.77	5.17E-05
	GOTERM_BP_DIRECT	GO:0006954~inflammatory response	14	8.19	7.07E-05
	GOTERM_BP_DIRECT	GO:0006898~receptor-mediated endocytosis	10	5.85	7.42E-05
	GOTERM_CC_DIRECT	GO:0005887~integral component of plasma membrane	49	28.65	1.26E-15
	GOTERM_CC_DIRECT	GO:0005615~extracellular space	42	24.56	8.63E-12
	GOTERM_CC_DIRECT	GO:0005886~plasma membrane	76	44.44	3.59E-10
	GOTERM_CC_DIRECT	GO:0005576~extracellular region	41	23.98	6.74E-09
	GOTERM_CC_DIRECT	GO:0009897~external side of plasma membrane	14	8.19	1.04E-07
	GOTERM_MF_DIRECT	GO:0005044~scavenger receptor activity	6	3.51	7.16E-05
	GOTERM_MF_DIRECT	GO:0015254~glycerol channel activity	4	2.34	1.51E-04
	GOTERM_MF_DIRECT	GO:0015250~water channel activity	4	2.34	3.75E-04
	GOTERM_MF_DIRECT	GO:0050544~arachidonic acid binding	3	1.75	8.02E-04
	GOTERM_MF_DIRECT	GO:0005372~water transmembrane transporter activity	3	1.75	0.001195295
	KEGG_PATHWAY	hsa04610:Complement and coagulation cascades	9	5.26	2.73E-06
	KEGG_PATHWAY	hsa04145:Phagosome	8	4.68	0.003357596
	KEGG_PATHWAY	hsa05150:Staphylococcus aureus infection	5	2.92	0.005263316
	KEGG_PATHWAY	hsa00350:Tyrosine metabolism	4	2.34	0.010477135
	KEGG_PATHWAY	hsa03320:PPAR signaling pathway	5	2.92	0.011220402

Table 2 Top 20 hub genes which were screened with degree more than 90

Top 20 hub genes which were screened with degree more than 90

Gene symble	Degree	Betweenness	Gene symble	Degree	Betweenness
TOP2A	112	0.11660323	AURKA	95	0.00363657
BUB1	103	0.01249734	MELK	95	0.0102998
CCNB1	103	0.01055831	RFC4	94	0.0142881
CCNA2	99	0.00526077	PBK	94	0.00957059
KIF11	99	0.00331167	BUB1B	93	0.00216013
NDC80	98	0.00388508	CDKN3	93	0.03636562
TTK	98	0.00316118	CDC6	92	0.0049405
CHEK1	97	0.00509206	CCNB2	92	0.00226211
NCAPG	96	0.00241139	DTL	92	0.00224199
ASPM	96	0.00537039	RACGAP1	91	0.00170142

Table 3 The functional annotation and enrichment of modules genes

The functional annotation and enrichment of modules genes

Module	Term	Count	PValue	FDR	Genes
module1	GO:0005515~protein binding	74	6.45E-15	7.65E-12	KIF23, STIL, PRC1, EZH2, KNTC1, TTK, AURKA, PTTG1, MCM10, KIF2C, CDCA8, TOP2A, CCNA2, CDCA5, KIF14, CDC6, DTL, KIF15, TPX2, NUSAP1, DEPDC1, MCM2, PBK, UBE2C, ECT2, MCM6, RFC5, RFC3, RFC4, SPAG5, RRM2, ZWINT, BUB1B, MELK, SHCBP1, KIF4A, BLM, NEK2, FOXM1, KIAA0101, CHEK1, CEP55, HMMR, SPC25, NCAPH, POLE2, NCAPG2, NCAPG, BUB1, FBXO5, ASF1B, POLQ, EXO1, RAD51AP1, MKI67, GMNN, KIF18A, NUF2, CENPF, NDC80, CENPE, CDC20, CDC25C, CENPK, RACGAP1, CDKN3, RAD54L, BRCA1, CCNB1, PLK4, CCNB2, PCNA, CKS2, KIF20A
	GO:0051301~cell division	33	3.32E-15	2.00E-29	NEK2, KNTC1, AURKA, PTTG1, SPC25, KIF2C, CDCA8, NCAPH, CDCA7, NCAPG2, NCAPG, CDCA2, BUB1, FBXO5, CCNA2, CDCA5, KIF14, CDC6, KIF11, TPX2, NUF2, CENPF, NDC80, CENPE, CDC20, CDC25C, UBE2C, CCNB1, CCNB2, SPAG5, ZWINT, CKS2, BUB1B
	hsa04110:Cell cycle	14	4.74E-15	3.87E-12	CDC6, TTK, CDC20, CHEK1, PTTG1, MCM2, CDC25C, MCM6, CCNB1, CCNB2, PCNA, BUB1, BUB1B, CCNA2
module2	GO:0006954~inflammatory response	6	3.97E-06	0.005450294	C5AR1, OLR1, PTGS2, C3, CCL21, CXCL2
	GO:0005886~plasma membrane	8	8.01E-03	7.548702693	CAV1, IL1R1, CD36, C5AR1, OLR1, C3, CXCL16, GNG11
	hsa04062:Chemokine signaling pathway	4	2.73E-03	2.697201033	CCL21, CXCL16, CXCL2, GNG11
module3	GO:0006968~cellular defense response	2	1.10E-02	10.66202665	NCF2, MNDA

Figures

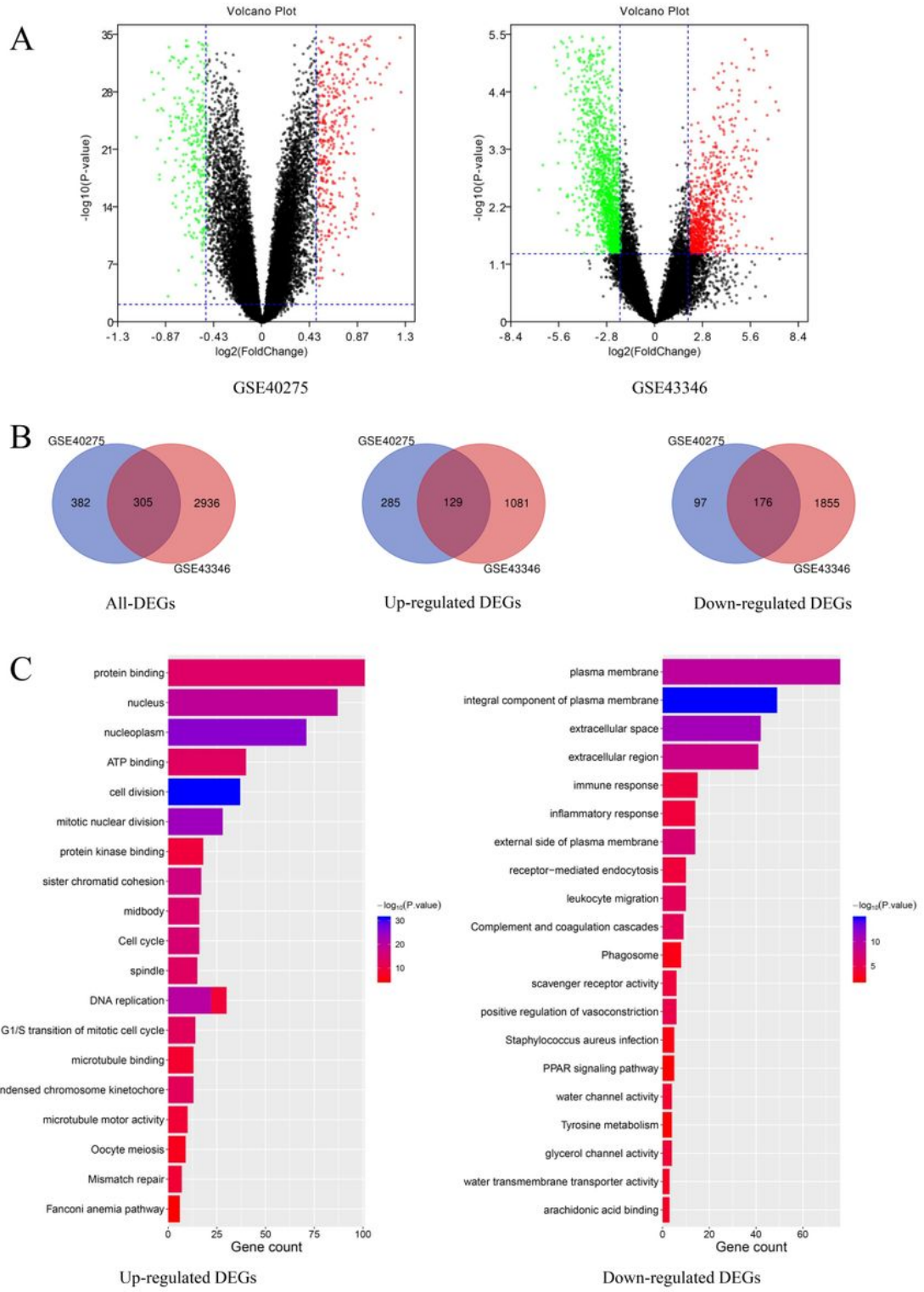

Figure 1

(A) The volcano plots of two datasets (B) The Venn plots of DEGs among two datasets (C) Functional and pathway enrichment analysis of up-regulated genes and down-regulated genes

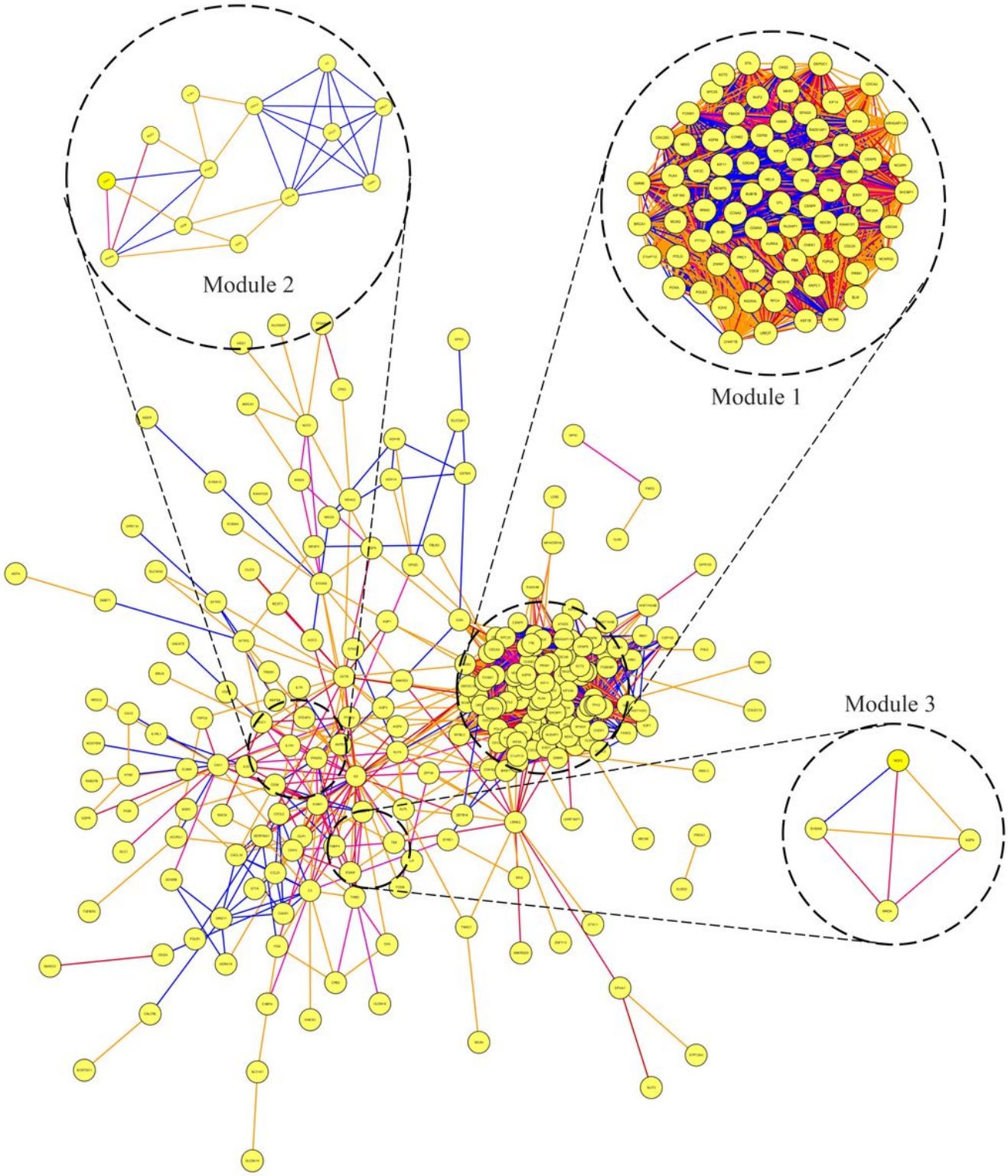

Figure 2

Top 3 modules from the protein-protein interaction network

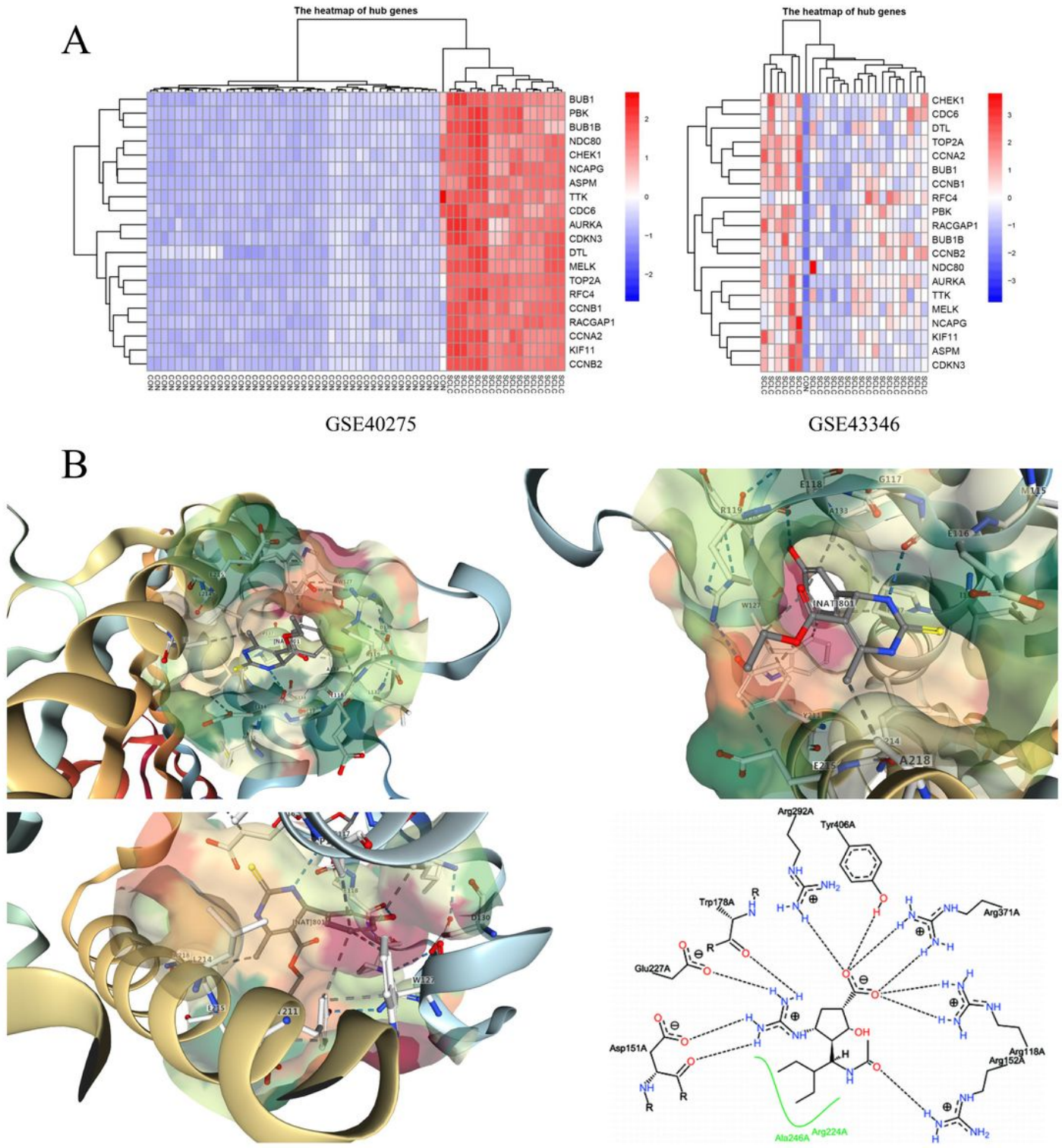

Figure 3

(A) Hub genes expression heat map of GSE40275 and GSE43346 (B) Binding of Monastrol to KIF11 protein

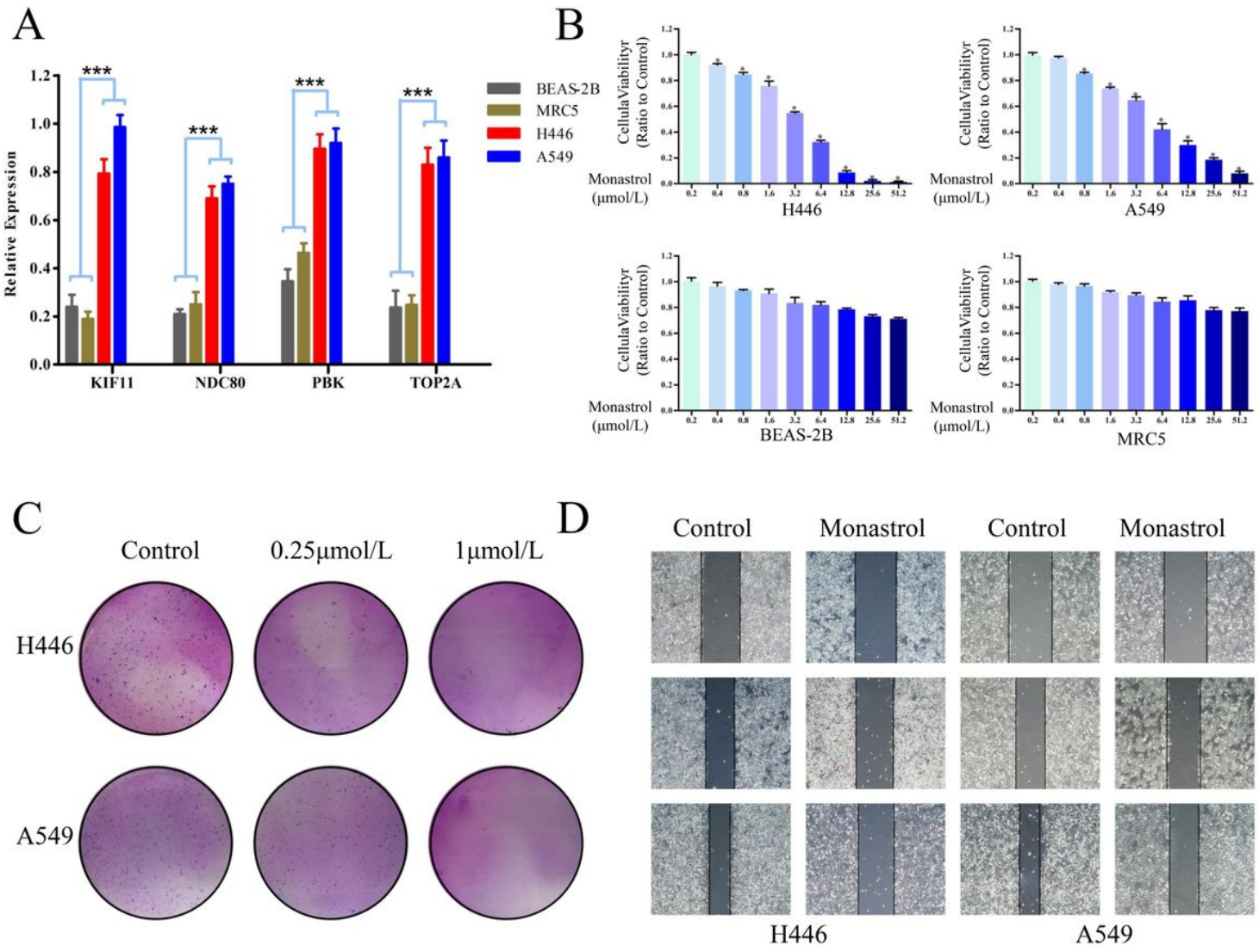

Figure 4

(A) Hub genes expression in different cell lines (B) Cellular viabilitys of different cell lines treated with Monastrol (C) Clonogenicities in Petri dishes with different doses of Monastrol (D) Scratch assay in control and Monastrol group